Author Manuscript

Author Manuscript

Author Manuscript

Author Manuscript

HHS Public Access

Author manuscript

Nature. Author manuscript; available in PMC 2021 September 03.

Published in final edited form as:

Nature. 2021 April ; 592(7853): 262–266. doi:10.1038/s41586-021-03299-4.

Hunger enhances food odor attraction through a Neuropeptide Y spotlight

Nao Horio, **Stephen D. Liberles***

Howard Hughes Medical Institute, Department of Cell Biology, Harvard Medical School, Boston, MA 02115, USA

Abstract

Internal state controls olfaction through poorly understood mechanisms. Odors signifying food, mates, competitors, and predators activate parallel neural circuits that may be flexibly shaped by physiological need to alter behavioral outcome[1]. Here, we identify a neuronal mechanism by which hunger selectively promotes attraction to food odors over other olfactory cues. Optogenetic activation of hypothalamic Agouti-Related Peptide (AGRP) neurons enhances attraction to food odors but not pheromones, with branch-specific activation and inhibition revealing a key role for projections to the paraventricular thalamus. Knockout mice lacking Neuropeptide Y (NPY) or NPY receptor type 5 (NPY5R) fail to prefer food odors over pheromones after fasting, with hunger-dependent food odor attraction restored by cell-specific NPY rescue in AGRP neurons. Furthermore, acute NPY injection immediately rescues behavior without additional training, indicating that NPY is required for reading olfactory circuits during behavioral expression rather than writing olfactory circuits during odor learning. Together, these findings show that food odor-responsive neurons comprise an olfactory subcircuit that listens to hunger state through thalamic NPY release, and more generally, provide mechanistic insights into how internal state regulates behavior.

The mouse olfactory system elicits myriad behaviors that include feeding, mating, fighting, and predator escape. Choice of behavioral action is strongly influenced by physiological need, yet mechanisms by which internal state sculpts olfactory circuits remain poorly defined. Hunger is a powerful motivational state that intensely drives behaviors predictive of food consumption[2,3]. In humans, hunger enhances the pleasantness rating of food odors[4], while in mice, starvation impacts general features of olfaction, such as arousal, sniffing rate and sensitivity to novel odors[5]. Here, we asked whether and how hunger might exert selective control over olfactory subcircuits that attend to food odors.

Users may view, print, copy, and download text and data-mine the content in such documents, for the purposes of academic research, subject always to the full Conditions of use:http://www.nature.com/authors/editorial_policies/license.html#termsReprints and permissions information is available at www.nature.com/reprints.

*Corresponding author: Stephen_Liberles@hms.harvard.edu, phone: (617) 432-7283, fax: (617) 432-7285.

Author Contributions

NH and SDL designed experiments, NH performed experiments, and SDL wrote the manuscript.

Competing interests declaration

The authors declare no competing financial interests.

Supplementary Information is available for this paper.

Author Manuscript Author Manuscript Author Manuscript Author Manuscript

Various odors activate discrete neuronal ensembles in the olfactory epithelium, olfactory bulb, and olfactory cortex[1]. In mouse, food odors and volatile sex pheromones are both attractive[1] but relevant for different physiological drives, suggesting that responsive neurons at some circuitry node display key differences, such as in connectivity, gene expression, and/or hormone responsiveness. Hunger-dependent modulation of olfactory inputs has been proposed to occur early in olfactory processing in vertebrates[5–7], and in other model organisms[8]. Satiety state alters the hedonic quality of food, but is not thought to impact the ability to recognize or detect food, which would be maladaptive for locating food stores for future use[4]. Thus, it is additionally possible that behaviorally relevant state-dependent modulation occurs through central pathways downstream of primary olfactory areas.

Hunger state guides odor responses

We used a simple and robust two-choice assay to investigate hunger-dependent odor responses. Mice were placed in a test arena containing volatile odor ports on each side without direct stimulus contact (Fig. 1a)[9]. Investigation time was quantified as the time in which the mouse's nose was directly above an odor port, and a preference index was calculated as the normalized difference in odor investigation times. Mice were attracted to both food odors (familiar homecage chow dissolved in water and centrifuged to remove insoluble debris) and pheromones (opposite sex mouse urine), compared with water (Extended Data Fig. 1). When paired against each other, food odors and pheromones were similarly attractive to fed mice; in contrast, fasted mice (males and females) displayed a strong preference for food odors over pheromones, with hunger promoting food odor investigation in two-choice comparisons or in single-odor pairings with water (Fig. 1b, Extended Data Fig. 1). Conversely, prior mate exposure increased attraction to volatile pheromones over food odors in fed but not fasted mice (Extended Data Fig. 2), consistent with need-based prioritization of behavior[10]. The observation that hunger enhances attraction to food odors relative to pheromones suggests that specific olfactory subcircuits can be differentially modulated by hunger-control centers in the brain.

A hypothalamus-to-thalamus circuit

Hypothalamic neurons expressing Agouti-Related Peptide (AGRP) help generate hunger drive. Optogenetic and chemogenetic activation of AGRP neurons in the arcuate nucleus powerfully motivates feeding behavior[11,12], while ablation of AGRP neurons in adult mice causes lethal starvation[13]. We therefore asked whether optogenetic activation of hypothalamic AGRP neurons alters odor preference behavior (Fig. 1c–e, Extended Data Fig. 3a–c). Optogenetic activation was achieved in *Agrp-ires-Cre* mice containing a Channelrhodopsin reporter allele (*lsl-ChR2*) using optic fibers implanted in the arcuate nucleus. Light stimulation in fed control mice (*Agrp-ires-Cre*) did not alter odor preference behavior, but in fed AGRP-ON mice (*Agrp-ires-Cre; lsl-ChR2*) light stimulation strongly enhanced behavioral attraction to food odors relative to pheromones, with a preference similar to that of fasted wild type mice. Thus, AGRP neurons promote behavioral attraction through some olfactory pathways but not others.

Author Manuscript Author Manuscript Author Manuscript Author Manuscript

Next, we asked whether AGRP neuron terminals in particular brain regions promoted food odor attraction (Fig. 2a). Collectively, AGRP neurons have widespread projections, and approaches involving terminal-specific optogenetics in AGRP neurons have revealed a striking division of labor among downstream targets[14–17]. Individual AGRP neurons can display selectivity among target areas, so branch-specific illumination does not cause antidromic activation of axon terminals in all other locations[15]. *Agrp-ires-Cre* (AGRP-ON) or wild type (control) mice were injected with a Cre-dependent adeno-associated virus (AAV) encoding Channelrhodopsin (*AAV-DIO-ChR2*) in the arcuate nucleus, and optic fibers were used to illuminate various brain areas that receive AGRP neuron input. Optogenetic stimulation of AGRP neuron terminals in the paraventricular thalamus (PVT), but not in other brain regions analyzed, promoted food odor attraction in fed AGRP-ON mice (Fig. 2b, Extended Data Fig. 3d–e), with similar responses in mice re-fed acutely after a fast or fed ad libitum (Extended Data Fig. 3f–h). Responses were of similar magnitude after somatic stimulation of AGRP neurons and were not observed in control mice lacking Cre (Fig. 2b). Optogenetic activation of AGRP terminals in other brain regions failed to induce food odor preference in fed mice (Fig. 2b, Extended Data Fig. 3d), including the bed nucleus of the stria terminalis (BNST), paraventricular hypothalamus (PVH), central nucleus of the amygdala (CeA), lateral hypothalamus (LH), medial amygdala (MeA), periaqueductal gray (PAG), and parabrachial nucleus (PBN). Interestingly, stimulating AGRP axons in BNST, PVH, and LH promoted robust food consumption in fed mice (Fig. 2c), as reported previously[15], but did not enhance food odor preference. Moreover, AGRP neurons that target the MeA and PBN suppress competing behaviors related to aggression and pain[14,17], but were also not involved in odor preference.

Since food odor perception can arise from experience, we asked whether novel odors could be entrained as food odors and subsequently evoke state-dependent responses (Extended Data Fig. 4). Food-restricted mice were given a diet of strawberry gelatin during a four-day training period. Before training, mice preferred pheromone odor to strawberry gelatin odor whether fed or fasted, but after training, mice displayed hunger-dependent attraction to strawberry gelatin odor. Furthermore, optogenetic stimulation of AGRP neuron terminals in the PVT promoted attraction to strawberry gelatin odor only after training.

Stimulating AGRP neuron projections to PVT promoted food odor attraction in fed mice, so we asked whether silencing these projections decreased food odor attraction in fasted mice. Expressing an inhibitory opsin, halorhodopsin, in AGRP neurons caused light-induced reductions in membrane potential and firing rate (Extended Data Fig. 5a). We inserted optic fibers in the PVT (PVT-OFF) or arcuate nucleus (ARC-OFF) of *Agrp-ires-Cre; lsl-halorhodopsin* mice or in control *Agrp-ires-Cre* mice. Illumination in fasted PVT-OFF or ARC-OFF mice but not in control mice lacking halorhodopsin decreased food odor attraction to levels seen in fed mice (Fig. 2d, Extended Data Fig. 5b, c), indicating that AGRP neuron projections to the PVT are required for hunger-dependent enhancement of food odor attraction. Despite similar odor preference responses, post-assay feeding was normal in fasted PVT-OFF mice, but reduced in fasted ARC-OFF mice (Extended Data Fig. 5d). The PVT is located dorsally within the thalamus, and intriguingly, in humans, attention to food odors engages the dorsal thalamus and amygdala[18], and patients with lesions in

Author Manuscript Author Manuscript Author Manuscript Author Manuscript

dorsal thalamus perceive food odors as neutral or aversive without losing their ability to identify them[19].

AGRP neurons display transient activity decreases upon food cue presentation[20,21]. We used fiber photometry to ask whether similar changes were observed in PVT-projecting AGRP axons. We injected the arcuate nucleus of *Agrp-Cre* mice with an AAV containing a Cre-dependent *GCaMP* allele, placed optic fibers in either the arcuate nucleus, PVT, or PVH, and recorded responses in fasted mice presented with food odors or pheromones (Extended Data Fig. 6). Food odor transiently inhibited AGRP neuron activity in all locations measured, while pheromones had no effect. Importantly, decreases in AGRP neuron activity were short-lived, while food odor attraction persisted throughout the behavioral assay. Moreover, optogenetic stimulation of AGRP neurons- not inhibition- promoted food odor attraction, while optogenetic inhibition of AGRP neurons, which was significantly longer than the transient activity decreases observed during food odor presentation, actually blocked fasting-induced food odor attraction. Presumably, the persistent stimulation of AGRP neurons that occurs during a fasted state enhances food odor attraction through sustained signaling in downstream neurons, perhaps through the durable action of a neuromodulator.

Roles for NPY and its receptor NPY5R

AGRP neurons release three principal neurotransmitters: AGRP, Neuropeptide Y (NPY), and γ-aminobutyric acid (GABA)[22], so we asked whether any was required for hunger-dependent odor attraction (Fig. 3a, b, Extended Data Fig. 7a–c). We obtained knockout mice lacking GABA in AGRP neurons (*Agrp-ires-Cre; Vgat-flox or GABA-KO*), NPY (*Npy-KO*), and melanocortin receptor 4 (*Mc4r-KO*), a receptor which mediates key physiological effects of hypothalamic AGRP. Strikingly, fasted *Npy-KO* mice did not prefer food odor over pheromones, while fasted *GABA-KO* and *Mc4r-KO* mice instead displayed normal hunger-dependent food odor attraction. When fed, attraction to food odors and pheromones was similar in *GABA-KO*, *Npy-KO*, *Mc4r-KO*, and wild type mice. Thus, fed *Npy-KO* mice retain a lower level of attraction to food odors that is comparable to pheromone attraction, but lose hunger-dependent enhancement of food odor preference. Mate exposure-dependent enhancement of pheromone attraction persisted in *Npy-KO* mice (Extended Data Fig. 2), suggesting other mechanisms of toggling pheromone-responsive olfactory circuits.

NPY is expressed in many neuron types, including AGRP neurons. We performed cell-specific NPY rescue to determine whether behavioral deficits observed in global *Npy-KO* mice were due to loss of NPY expression in AGRP neurons[23]. A Cre-dependent AAV encoding NPY (*AAV-DIO-Npy*) was injected into the arcuate nucleus of *Agrp-ires-Cre*; *Npy-KO* (Npy^{AGRP} rescue) or *Npy-KO* (control) mice. Rescue of NPY expression in AGRP neurons restored hunger-dependent food odor attraction (Fig. 3c–d, Extended Data Fig. 7d), indicating that AGRP neuron-derived NPY is sufficient for state-dependent modulation of food odor responses.

NPY receptors comprise a small subfamily of five G Protein-Coupled Receptors. To determine whether a particular NPY receptor was responsible, we obtained knockout mice

Author Manuscript Author Manuscript Author Manuscript Author Manuscript

lacking individual NPY receptors and tested odor preference behavior (Fig. 3e–f, Extended Data Fig. 7e–g). Fasted male and female *Npy5r-KO* mice failed to prefer food odors to pheromones, despite normal hunger-dependent food consumption, while fasted *Npy1r-KO* mice displayed normal odor preference behavior. Like *Npy-KO* mice, *Npy5r-KO* mice displayed attraction to food odor over water in the fed state, but lost hunger-dependent enhancement of this response (Extended Data Fig. 8). Hunger also promoted search for food buried in bedding, and food search behavior was impaired in fasted *Npy-KO* and *Npy5r-KO* mice (Extended Data Fig. 9a). Together, these findings reveal an essential role for both a neuropeptide, NPY, and its receptor, NPY5R, in hunger-evoked odor attraction.

RNA *in situ* hybridization experiments revealed detectable *Npy5r* expression in cortical regions including the olfactory cortex but not the PVT (Extended Data Fig. 9b, c). One possibility is that NPY5R is localized to incoming cortical axons that arrive in dorsal thalamus. PVT injections of NPY5R antagonists blocked food odor attraction in fasted mice, while PVT injections of NPY5R agonists promoted food odor attraction in *Npy* knockout mice (Fig. 3g–i, Extended Data Fig. 10a–b). Similar agonist injections into the dorsal third ventricle just above the PVT had no effect, although injecting higher agonist concentrations into the ventral third ventricle an hour before behavioral assessment enhanced food odor attraction, presumably because sufficient agonist could then access the PVT (Extended Data Fig. 10c–d). Together, pharmacological and optogenetic studies indicate that AGRP neuron-derived NPY5R agonism within the PVT underlies hunger enhancement of food odor attraction.

In mice, perception of food odors can arise through learning (Extended Data Fig. 4). Thus, loss of hunger-evoked food odor preference in both *Npy-KO* and *Npy5r-KO* mice could be explained by deficits in either memory formation or hunger-induced behavioral expression, or both. AGRP neurons provide a negative valence teaching signal[20], and in *Drosophila*, an NPY homolog is required for appetitive memory performance[24]. If NPY were required for formation of food odor memory, then re-administration of NPY in *Npy-KO* mice would not restore hunger-dependent food odor preference until learning could subsequently occur. We observed that injection of NPY, or a specific NPY5R agonist, into fasted *Npy-KO* mice immediately restored hunger-dependent food odor preference in the absence of additional training (Fig. 3g–i). Mice had learned particular olfactory cues to be food-associated in the absence of NPY, likely explaining the persistent basal attraction to food odor (comparable to pheromone attraction) observed in fed *Npy-KO* mice. Thus, NPY acts in the expression of hunger-enhanced food odor attraction rather than the formation of food odor memory.

Discussion

Many pathways have been proposed by which nutrients and feeding-relevant hormones may interact with the olfactory system. Here, we reveal an essential role for NPY and its receptor NPY5R in hunger-dependent odor preference. AGRP neurons that project to the PVT provide a key first connection from hunger neurons to olfactory circuits. Olfaction has been considered unique among the senses in that olfactory inputs largely access cortical regions without traversing the thalamus[25], although a minor output pathway of the piriform cortex involves the medio-dorsal thalamic nucleus[26], which is adjacent to the PVT. In addition, top-

Author Manuscript Author Manuscript Author Manuscript Author Manuscript

down olfactory inputs, such as from prefrontal cortex, descend on PVT[27], where they presumably can be integrated with information about hunger state from AGRP neurons. Interestingly, the PVT gates information from other states, including thirst[28], and from other sensory systems, including visual cues[29], and may generally guide attention to salient inputs relevant for a current behavioral state. The PVT additionally plays a role in withdrawal symptoms associated with drug addiction[30], consistent with a function in enhancing the valence of environmental cues that alleviate negative stressors, like hunger, thirst, and drug craving.

Neuromodulation that controls the relative strength of signals through different sensory channels allows for flexible behaviors that vary with need. Here we uncover molecular features essential for one such neuromodulatory pathway, as NPY from AGRP neurons opens a thalamic hunger gate for specific olfactory inputs carrying an NPY5R encryption. It seems likely that different neurotransmitters function as spotlights for other behavioral drives, with the thalamus serving a general role as a switchboard that gates preferential attention to sensory inputs based on physiological need.

Methods

Animals.

All animal procedures followed the ethical guidelines outlined in the NIH Guide for the Care and Use of Laboratory Animals, and all protocols were approved by the institutional animal care and use committee (IACUC) at Harvard Medical School. Animals were maintained under constant temperature (23 ± 1°C) and relative humidity (46 ± 5%) with a 12-h light/dark cycle. Wild type C57BL/6 (000664), *Agrp-ires-Cre* (012899), *lsl-ChR2* (024109), *lsl-Halorhodopsin* (014539), *Mc4r-KO* (006414), *Vgat-flox* (012897), *Npy-KO* (004545), *Npy1r-KO* (005408) and *Npy5r-KO* (007584) mice were purchased (>8 weeks old; Jackson).

Two-choice odor preference test.

Odor preference was measured using a described two-choice paradigm[9] with minor modifications. The test arena consisted of two odor applicators placed on each side of a plastic cage (M-BTM-STD, Innovive) without bedding. Odor applicators were petri dishes (35 mm, Falcon, 351008) with thirteen holes drilled in the lid to enable odor escape. Test stimuli or water (400 μl) water were added just prior to testing, and the petri dish lid was closed to prevent direct stimulus contact. Food odor was prepared by suspending 20 g of normal chow (LabDiet 5058, Lab Supply) in 50 ml water (4 hours) and centrifuging (1000 rpm, 5 min) to remove insoluble material; mouse urine was freshly collected by hand. Mice were individually housed, naive to the paradigm, and tested in the dark phase. Fed and fasted mice were fasted for 24 hours, and immediately prior to testing, fed mice were given free access to food for one hour while fasted mice were not; mice fed ad libitum were never food restricted. Mate-exposed mice lived with a mate for 24 hours immediately prior to isolation for fasting. Mice were habituated by successive administration (3 × 5 min) to mock test arenas containing blank odor applicators, and then introduced into the test arena. Odors were placed on each side of the arena in different tests, and no side bias was observed in control

Author Manuscript Author Manuscript Author Manuscript Author Manuscript

experiments involving water alone (Extended Data Fig. 1b). Mice were recorded with a digital video camera, and odor investigation scored manually, in a randomized double-blind manner, as time investigating each petri dish over the entire test period (5 min). The position of the mouse nose was illustrated in Figure 1 using Optimouse software[32]. Investigation time was quantified as the time in which the mouse's nose was directly above an odor port, and preference index was calculated as the percentage of time investigating food odor minus the percentage of time investigating pheromones. Data from rare mice were excluded if they did not investigate both odor sources during the two-choice odor test. Statistical analysis was performed using a Wilcoxon matched-pairs signed rank test. Sample sizes were based on prior publications involving two-choice odor tests[9].

Food intake measurement.

Food intake was measured just before or after odor preference tests, as indicated in figure timelines. Food and water were provided ad libitum in a clean cage, and the amount of food consumed over 1 hour was measured by weighing food before and after the test period.

Optogenetics.

For surgical injection of AAV and implantation of optic fibers, mice were anesthetized with avertin (250 mg/kg) and placed into a stereotaxic device (KOPF). After exposing the skull via small incision, a small hole was drilled. For axonal activation of AGRP neurons, *AAV-DIO-ChR2* (Addgene 20297-AAV9, titer: 3.1×10^{13} genomes/ml) was injected bilaterally into the arcuate nucleus (bregma −1.45 mm, midline ± 0.20 mm, skull surface −5.95, −5.85, −5.75 mm, 50 nl per site) of *Agrp-ires-Cre* mice using a pulled-glass pipette with 20–40 μm tip diameter. A micromanipulator (Nanoject III, Drummond) was used to control injection speed and volume, and the pipette was withdrawn 5 min after injection. Optic fibers (200 μm core, NA 0.50, Thorlabs) with a ferrule (Thorlabs) were implanted unilaterally in either the arcuate nucleus (bregma −1.45 mm, midline ± 0 mm, skull surface −5.6 mm), BNST (bregma +0.62 mm, midline +0.65 mm, skull surface −4.40 mm), PVH (bregma −0.94 mm, midline ±0 mm, skull surface −4.80 mm), PVT (bregma −1.10 mm, midline ±0 mm, skull surface −3.20 mm), CeA (bregma −1.10 mm, midline +2.60 mm, skull surface −4.35 mm), LH (bregma −1.30 mm, midline +1.00 mm, skull surface −5.00 mm), MeA (bregma −1.60 mm, midline +2.00 mm, skull surface −5.50 mm), PAG (bregma −4.50 mm, midline +0.50 mm, skull surface −2.80 mm), or PBN (bregma −5.20 mm, midline +1.25 mm, skull surface −3.20 mm). Fibers were secured to the skull with dental cement and both fibers and ferrules covered with caps (Thorlabs) for protection. Mice recovered from optic fiber surgery for 1 week, and from AAV injection with optic fiber surgery for 3 weeks. Optogenetic protocols were similar to previous reports[15], and were initiated before the first habituation, and maintained for the duration of the odor preference test and subsequent food intake test. Light was delivered (10 ms pulses, 20 pulses for 1 sec, repeated every 4 seconds for activation or 1.5 seconds for inhibition, 6–8 mW to AGRP neuron soma and 6–10 mW to AGRP neuron axons) by LED (473 nm for activation, 625 nm for inhibition, Prizmatix) using a pulser (Prizmatix) through an optic fiber attached to the ferrule-capped optic fiber implanted in the mouse. Fiber placements were verified after each test by immunohistochemistry for AGRP (Neuromics GT15023, 1:100) and AAV injection sites were verified using AAV-derived mCherry fluorescence. Halorhodopsin function in AGRP neurons was validated by whole-

Author Manuscript Author Manuscript Author Manuscript Author Manuscript

cell current clamp recordings during optogenetic experiments (625 nm, 10 second continuous illumination, fiber output: 6–8 mW) of acutely harvested and dissociated arcuate nucleus two hours after attachment using a Molecular Device 700B amplifier with filtering at 1 kHz and 4–10 mΩ electrodes filled with an internal solution containing (in mM) 130 K-Gluconate, 15 KCl, 4 NaCl, 0.5 CaCl2, 10 HEPES, 1 EGTA, pH 7.2, 290 mOsm, with cells bathed in an external solution containing (in mM) 150 NaCl, 2.8 KCl, 1 MgSO4, 1 CaCl2, 10 HEPES, pH 7.4, 300 mOsm.

Food odor learning paradigm.

Prior to training, mice were food-restricted (2 g chow/day in food bowl to maintain 85–95% body weight) for four days. For training (next four days), food-restricted mice were given strawberry sugar-free gelatin[20] (Conagra Brands, Snack Pack) ad libitum in a food bowl for 30 minutes once a day (dark period). After gelatin was removed, mice were left without food for 1 hour, and then given 2.5 g chow/day (to maintain 80–90% body weight) to eat freely until the next day's training period. After the last day of training, mice were fasted as part of the two-choice odor test protocol instead of being given 2.5 g chow. During odor testing, strawberry gelatin (1 g) was placed in the odor applicator. In the pre-test trial when fasted (see Extended Data Fig. 4c), all mice were confirmed to prefer strawberry gelatin odor after training. For optogenetics experiments, training occurred three weeks after optic fiber placement.

Cell-specific NPY rescue.

Plasmid to generate *AAV-DIO-Npy* was made by insertion of an *Npy-mCherry* gene (excised from Addgene 67156 with NheI and BsrGI) into an AAV vector (*pAAV-EF1a-DIO-hM3D(Gq)-mCherry*, Addgene 50460 cut with NheI and BsrGI, which removes *hM3D(Gq)-mCherry*). *AAV-DIO-Npy* was produced in HEK-293T cells with a particular capsid (*AAV-PHP.eB*, Addgene 103005) and AAV helper (Addgene 112867). *AAV-DIO-NPY* (titer: 10^{13} genomes/ml) was injected bilaterally into the arcuate nucleus (bregma −1.45 mm, midline ± 0.20 mm, skull surface −5.95, −5.85, −5.75 mm, 50 nl per site) of *Npy-KO* or *Agrp-ires-Cre; Npy-KO* mice. Behavioral analysis was performed three weeks after AAV injection, and NPY expression was verified post-hoc by immunohistochemistry for NPY (Peninsula Laboratories, 1:250, T-4070.0050).

Administration of NPY5R ligands.

An external cannula (26 gauge, Plastics One) and dummy internal cannula were implanted into the PVT (bregma −1.10 mm, midline ±0 mm, skull surface −2.20 mm), dorsal third ventricle (bregma −1.10 mm, midline ±0 mm, skull surface −1.50 mm), or ventral third ventricle (bregma −1.30 mm, midline ±0 mm, skull surface −4.70 mm) and secured to the skull with dental cement. For injections, the dummy cannula was removed and an internal cannula (33 gauge, Plastics One) inserted 1 mm beyond the external cannula for a final distance from skull surface of −3.20 mm (PVT), −2.50 (dorsal third ventricle), or −5.70 (ventral third ventricle). Test stimuli were injected by syringe (0.02 µl/min) and included artificial cerebrospinal fluid (aCSF, TORCIS) alone, NPY (7.7 µg/µl in aCSF, 0.02 mg/kg except for ventral third ventricle injections in Extended Data 10 which involved 0.2 mg/kg, Bachem), NPY5R agonist ([CPP$^{1–7}$, NPY$^{19–23}$, Ala^{31}, Aib^{32}, Gln^{34}]-hPancreatic

Author Manuscript Author Manuscript Author Manuscript Author Manuscript

Polypeptide, 0.71 μg/μl in aCSF, 0.002 mg/kg, TOCRIS), and NPY5R antagonist (CGP71683 hydrochloride, 51.7 μg/μl in aCSF, 0.2 mg/kg, TOCRIS). After injection (1 min later), the internal cannula was removed and the dummy cannula re-inserted. Injections were performed immediately before habituation onset, except ventral third ventricle injections in Extended Data 10 were performed 45 minutes before habitation onset. Cannula placements were verified by histology.

Fiber photometry.

For fiber photometry, *Agrp-ires-Cre* mice were injected in the arcuate nucleus with *AAV-DIO-GCaMP6s* (Addgene #100845-AAV9, titer 2.1×10^{13} genomes/ml), and a patch fiber (200 mm core diameter, 0.57 NA, metal ferrule, Doric) was inserted in the arcuate nucleus, PVT, or PVH. Two weeks after surgery, fiber photometry was performed using an RZ10x real-time processor (Tucker-Davis Technologies). Light from connected 405 nm and 465 nm LEDs was filtered through a fluorescence minicube (Doric Lenses) and collected with an integrated photosensor on the RZ10x connected to the surgically implanted optic fiber with a 0.48 NA, 200 μm core diameter patchcord (Doric Lenses). Fiber photometry was performed on fasted mice during a one-choice odor preference assay, which involved habituation (3 × 5 min), a water test (5 min), rest (2 min in habituation chamber), a pheromone test (5 min), rest (2 min in habituation chamber), and food odor test (5 min). 10 minutes after the food odor test, mice were given direct access to food in their home cage during fiber photometry. Changes in calcium-dependent GCaMP6s fluorescence (465 nm) signal were compared with calcium-independent GCaMP6s fluorescence (405 nm), providing an internal control for movement and photobleaching artifacts. Fluorescence measurements were made, extracted from Synapse software (Tucker-Davis Technology), and analyzed in MATLAB (GraphPad). Fluorescence signal (F) was defined as the ratio of fluorescence measured at 465 nm divided by fluorescence measured at 405 nm; a delta F/F was expressed by comparing fluorescence signal to a pre-test baseline, and a mean delta F/F was calculated for time intervals indicated in figures. Statistical analysis was performed using TWO-way-ANOVA, then post-hoc Bonferroni's multiple comparisons test; mice were excluded from analysis if AGRP neurons did not respond during food consumption after the odor test and/or if GCaMP expression/ optic fiber placement was not properly targeted based on post-hoc histology.

Food search behavior.

Mice were fasted (24 hours) or fed ad libitum, and briefly removed from their home cage to a fresh cage. While mice were absent from the home cage, a food pellet (3 g) was buried beneath bedding (>1 cm), and the mice were then re-introduced to the home cage. The latency to discover the food was recorded, and if the food was not discovered within 10 minutes, the trial was ended, and the latency recorded as 600 seconds.

Single-color RNA in situ hybridization.

Coronal cryosections (16 μm) of freshly frozen mouse brain were washed with PBS, treated with proteinase K [Thermo Fisher Scientific, 10 mg/ml, 10 mM Tris-Cl (pH 7.4) with 1 mM EDTA (pH 8.0),10 min, 37°C], fixed (4% PFA, PBS, 10 min), washed (PBS, 5 min), acetylated (0.25% acetic anhydride, 1.3% triethanolamine, 0.25% HCl, in water, 10 min), washed (PBS, 5 min), dried, and pre-hybridized (60°C, 1 hour) in hybridization buffer [50%

Author Manuscript Author Manuscript Author Manuscript Author Manuscript

formamide, 0.6 M NaCl, 10 mM Tris-Cl (pH 8.0), 5 mM EDTA, 0.3 mg/ml yeast-tRNA, 1x Denhalt's solution, 0.1 mg/ml Heparin, 0.1% Tween-20, 0.25% SDS, in DEPC-treated water]. Digoxigenin-labeled cRNA probes were transcribed using T3 RNA polymerase from PCR-derived DNA templates amplified using the following primer pairs: *Npy5r-antisense* (899 bp) TGCCATTCCTTCAGTGTGTATC and AATTAACCCTCACTAAAGGGGGACATCATGCCTAACAAGTGA, *Npy5r* sense (899bp): AATTAACCCTCACTAAAGGGTGCCATTCCTTCAGTGTGTATC and GGACATCATGCCTAACAAGTGA, treated with DNase I (Roche Applied Science, 20 min, 37°C) and purified (ProbeQuant G-50 Columns, GE Healthcare). RNA probe (1.5 ng/μl in hybridization buffer) was preheated (85°C, 5 min), cooled on ice, and applied to each slide (200 μl beneath parafilm in a chamber equilibrated with 50% formamide, 16 hours, 60°C). Sections were washed [1: 5x SSC (3 min, 65°C), 2: 2x SSC/50% formamide (20 min, 65°C), 3: 0.2x SSC (2×20 min, 65°C)], blocked (1 hr, RT) in blocking buffer [1% blocking reagent (Roche Applied Science, 11096176001), 100 mM maleic acid, pH 8.0, 150 mM NaCl, 0.3% Tween-20], and incubated with primary antibody [horseradish peroxidase conjugated anti-Digoxigenin antibody (Roche Applied Science 11207733910), 1:500 in blocking buffer, overnight, 4°C]. On the next day, slides were washed (3 ×10 min, PBST), treated with TSA-plus Cyanine 3 (PerkinElmer, NEL744001KT,1:70 in 1x plus amplification diluent, 20 min), washed (1× 10 min, PBST) mounted with cover glass using Fluoromount with 4',6-diamidino-2-phenylindole dihydrochloride (Southern BioTech 0100–20), and analyzed by fluorescence microscopy.

Data availability.

All raw datapoints used for statistical analysis (Prism software) and to generate graphs are reported directly in Figures and also provided in Supplemental Source Data. Exact p values for pairwise data comparisons in Figures from left to right, using tests described in Figure Legends, are 1b: .85, .002; 1d: .77, .002; 2b (control): .82, .69, .44, .56, .69, .69, .69, .56, .77; 2b (AGRP-ON): .38, .69, .008, .57, >.99, .16, .69, .31, .002; 2c: .0003, .0007, .0004, .29, .89, .34, .59, <.0001; 2d: .03, .84; 3b (fed): .23, .38, .56; 3b (fasted): .002, .002, .63; 3d: .30, .0005; 3e:.002; .85; 3h: >.99, .03, .03; 3i: .03, .84.

Author Manuscript Author Manuscript Author Manuscript Author Manuscript

Extended Data

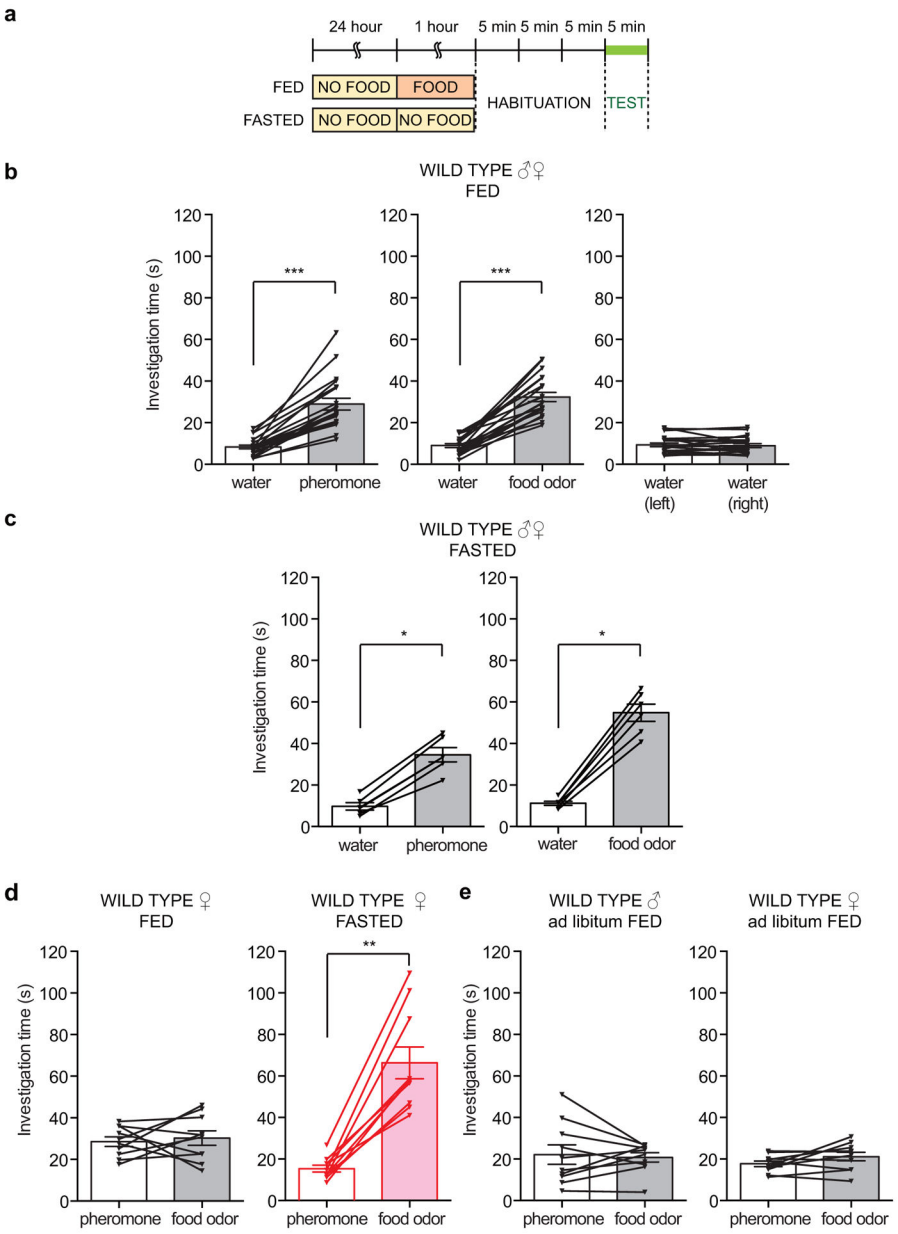

Extended Data Figure 1. Controls for two-choice odor preference assay.

a, Timeline of two-choice behavioral assay. **b-c**, Odor investigation times of fed (**b**) and fasted (**c**) male and female wild type mice in single odor pairings with water. (n=10 males and 10 females for **b**, 3 males and 3 females for **c**, mean ± s.e.m, lines with triangles: individual mice, *p<.05, ***p<.001 by two-tailed Wilcoxon test (p left to right in **b**: <.0001, <.0001, .86; p left to right in **c**: .03, .03). A statistical comparison of odor responses in **b** and **c** using a two-tailed Mann-Whitney *U* test revealed significant increases in food odor investigation in fasted mice compared with fed mice (p=.0006) but not in pheromone investigation (p=.15). **d**, Odor investigation times of fed (left) and fasted (right) wild type females, n=10 mice, mean ± s.e.m, lines with triangles: individual mice, **p<.01 by two-

Author Manuscript Author Manuscript Author Manuscript Author Manuscript

tailed Wilcoxon test (p fed: .77, p fasted: .002), **e**, Odor investigation times of male (left) and female (right) wild type mice fed ad libitum, n=10 mice, mean ± s.e.m, lines with triangles: individual mice, p values by two-tailed Wilcoxon test: male=.92, female=.19.

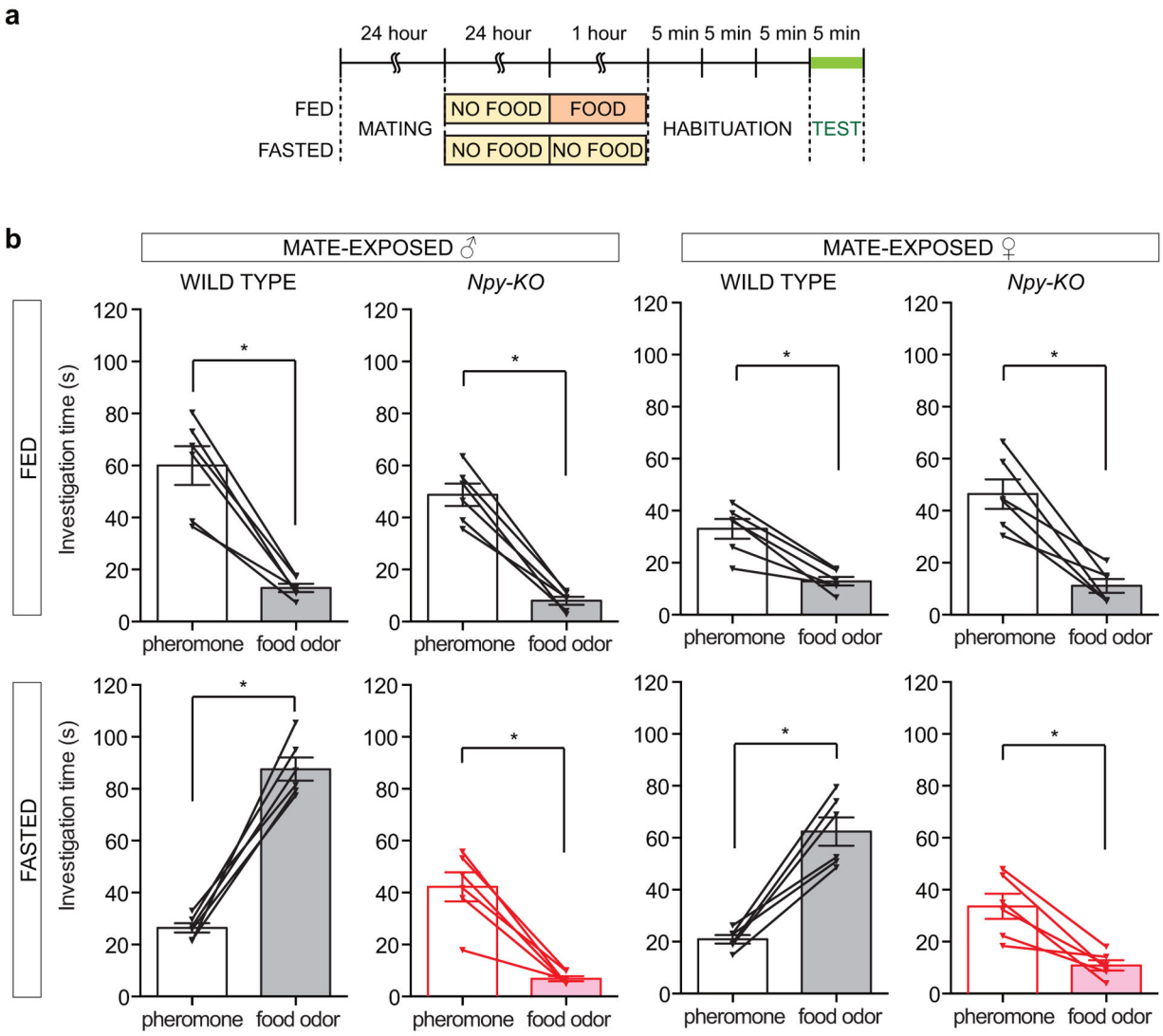

Extended Data Figure 2. Mate encounters selectively enhance pheromone attraction in fed mice through an NPY-independent mechanism.

a-b, Timeline of two-choice behavioral assay (**a**) and odor investigation times (**b**) after mate exposure, fed (top) and fasted (bottom), male (left) and female (right), wild type and *Npy-KO* mice, n=6 mice, mean ± s.e.m, lines with triangles: individual mice, *p<.05 by two-tailed Wilcoxon test (p left to right, fed: .03, .03, .03, .03; p left to right, fasted: .03, .03, .03, .03).

Author Manuscript Author Manuscript Author Manuscript Author Manuscript

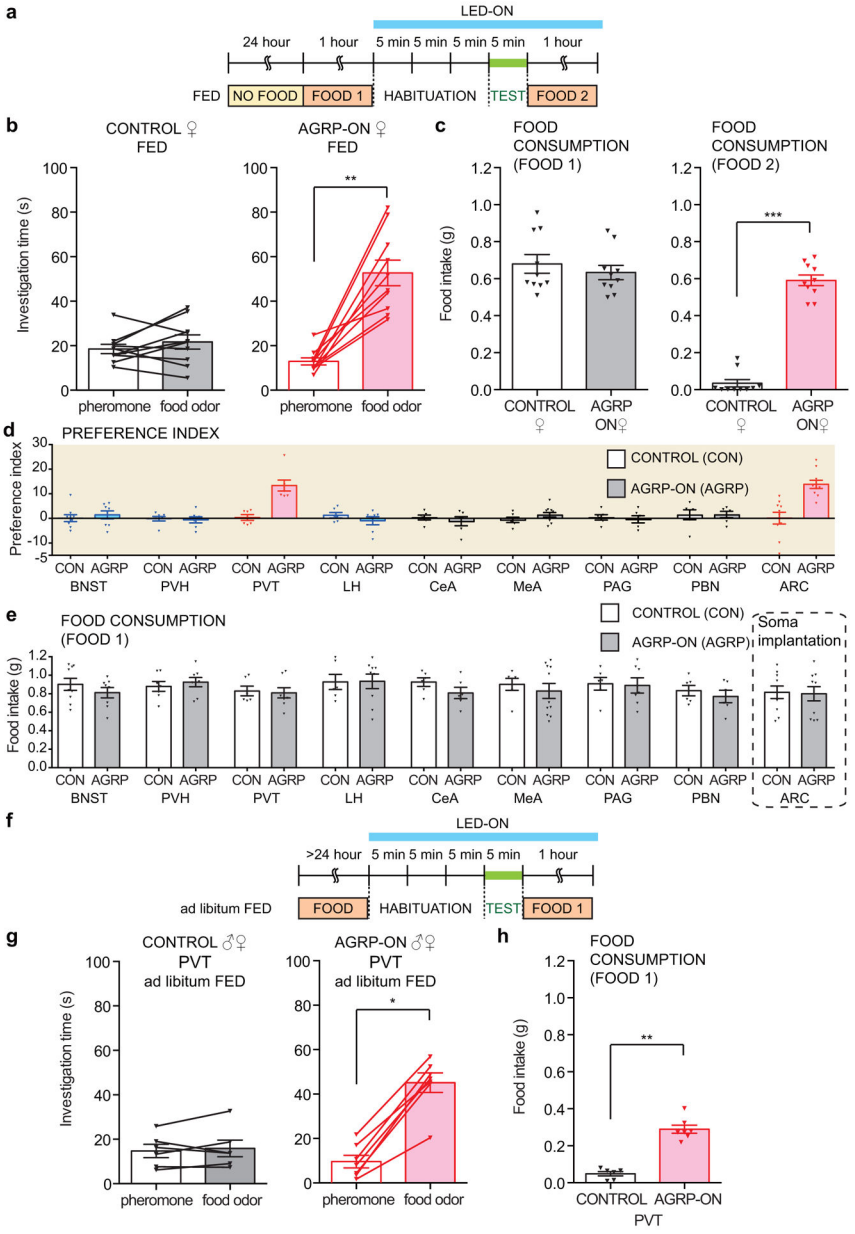

Extended Data Figure 3. Controls for experiments involving optogenetic stimulation of AGRP neuron projections to the PVT.

a, Timeline of two-choice assay involving optogenetic stimulation (blue bar) of AGRP neurons. **b**, Investigation time of fed control (black) and fed AGRP-ON (red) female mice to pheromones and food odors, n=10 mice, mean ± s.e.m, lines with triangles: individual mice, **p<.01 by two-tailed Wilcoxon test (p control: .32; p AGRP-ON: .02). **c**, Food intake was measured before (FOOD 1) and after (FOOD 2) the odor preference assay, as indicated in the timeline, for female mice used in **b**, n=10 mice, mean ± s.e.m, triangles: individual mice, ***p<.001 by Mann–Whitney *U* test (p FOOD1: .49; p FOOD2: <.0001). **d**, Preference index was calculated for fed control (unfilled bars, 'CON') and fed AGRP-ON (filled bars, 'AGRP') mice following illumination of brain regions indicated (n as reported for same mice in Fig. 2b–c, mean ± s.e.m). **e**, Food intake prior to two-choice assay and optogenetic

Author Manuscript Author Manuscript Author Manuscript Author Manuscript

stimulation (FOOD 1 in timeline) of mice with optic fibers implanted in various brain regions (n as reported for same mice in Fig. 2b–c, mean ± s.e.m, p values by Mann–Whitney *U* test from left to right: .47, .52, .90, .94, .18, .95, .81, .57, .89). **f**, Timeline of two-choice behavioral assay involving optogenetic stimulation (blue bar) of AGRP neurons in mice fed ad libitum. **g-h**, *AAV-DIO-ChR2* was injected in the arcuate nucleus of wild type (control) or *Agrp-ires-Cre* (AGRP-ON) mice, and optic fibers were inserted in PVT. Odor investigation times in the two-choice behavioral assay (**g**) and post-test food consumption (**h**, FOOD 1 from timeline in **f**) from indicated mice fed ad libitum, n=6 (control) and 7 (AGRP-ON) mice, mean ± s.e.m, lines with triangles: individual mice, *p<.05, **p<.01 (p values by two-tailed Wilcoxon test in **g**: .56, .02; p value by two-tailed Mann–Whitney *U* test in **h**: .0012).

Author Manuscript Author Manuscript Author Manuscript Author Manuscript

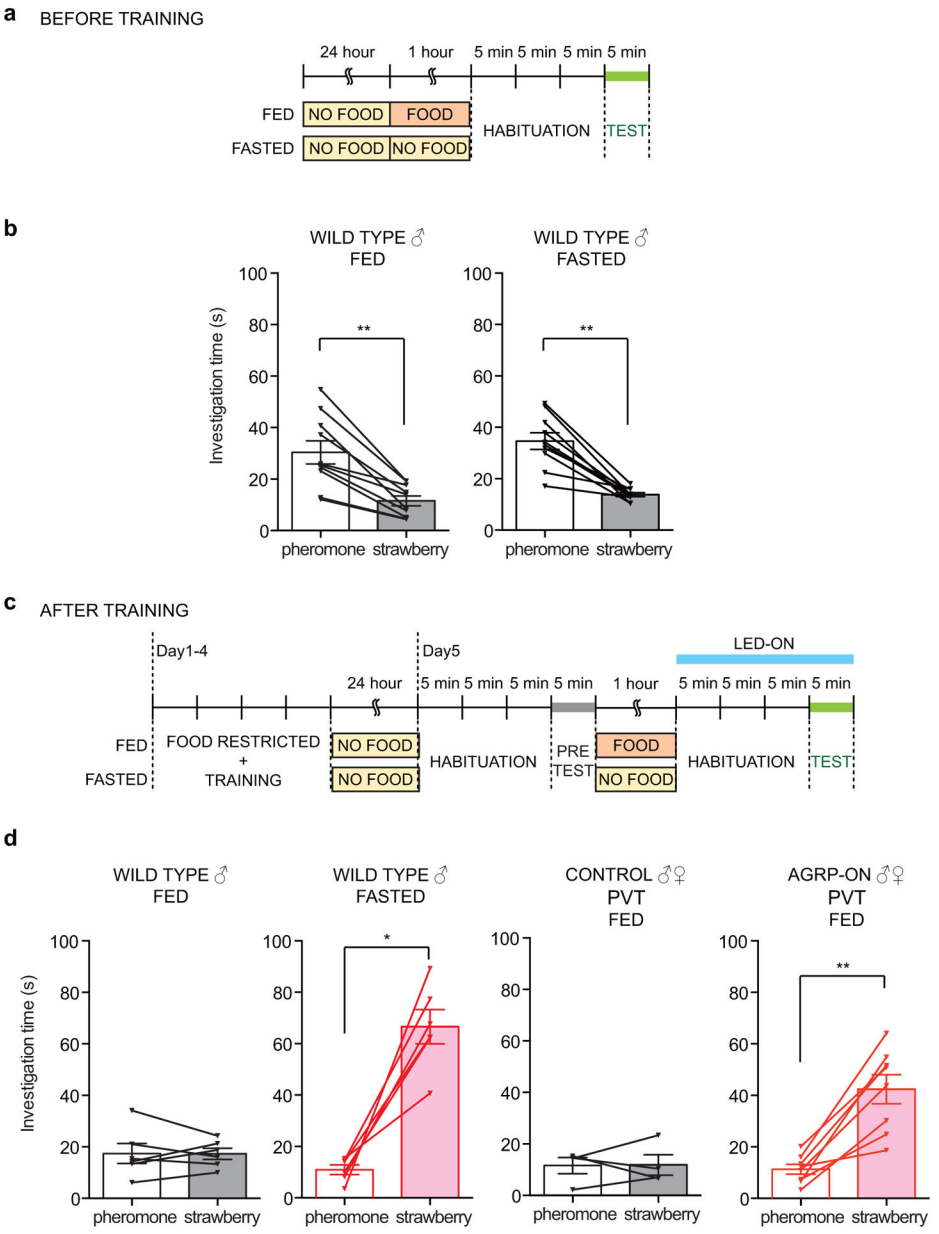

Extended Data Figure 4. Attraction to a newly learned food odor is enhanced by hunger and optogenetic stimulation.

a, Timeline of two-choice behavioral assay before learning. **b**, Investigation time of fed (left) and fasted (right) wild type male mice to pheromones (unfilled bars) and strawberry gelatin odor (filled bars) before learning, n=10 mice, mean ± s.e.m, lines with triangles: individual mice, **p<.01 by two-tailed Wilcoxon test (p fed: .002; p fasted: .002). **c**, Timeline of learning paradigm and two-choice behavioral assay after learning. **d**, Investigation time to pheromones (unfilled bars) and strawberry gelatin odor (filled bars) after learning in wild type fed, wild type fasted mice, wild type fed mice after arcuate nucleus injection of *AAV-DIO-ChR2* and PVT illumination (control), and *Agrp-ires-Cre* fed mice after arcuate nucleus injection of *AAV-DIO-ChR2* and PVT illumination, n=6 mice (wild type fed, fasted), 4 (control, PVT) and 8 (AGRP-ON, PVT), mean ± s.e.m, lines with triangles:

Author Manuscript Author Manuscript Author Manuscript Author Manuscript

individual mice, *p<.05, **p<.01 by two-tailed Wilcoxon test (p values from left to right: >.99, .03, .88, .008).

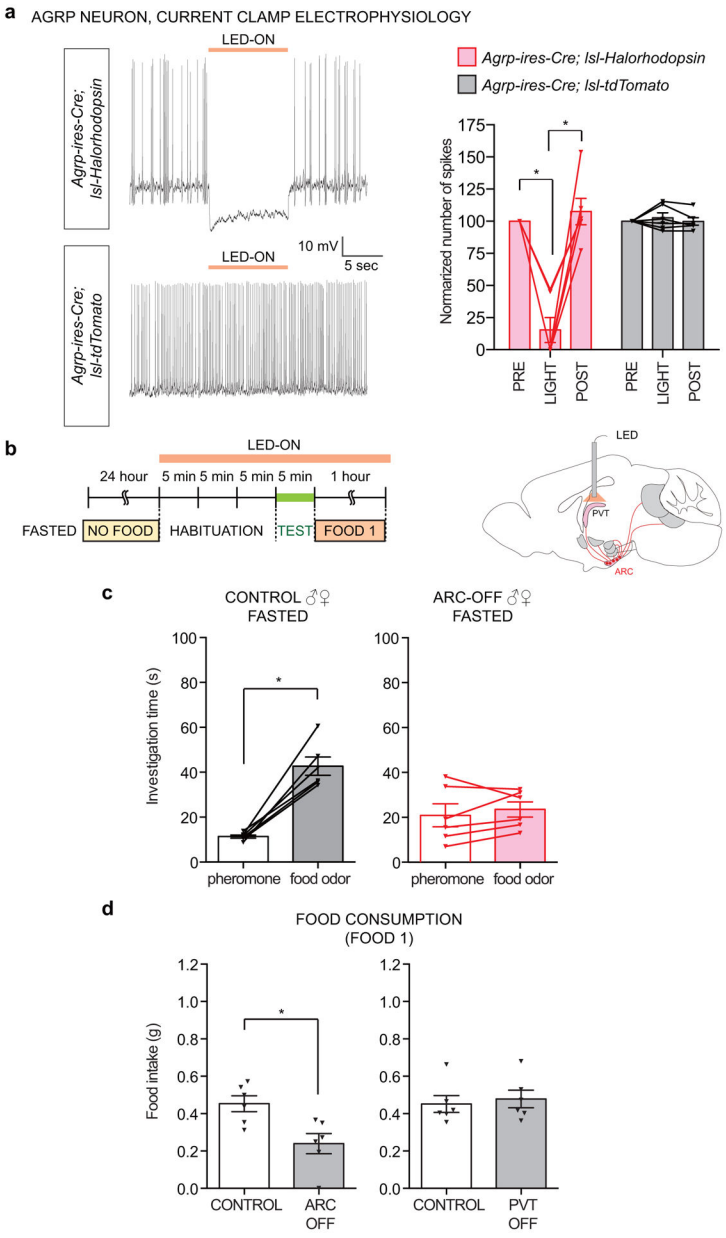

Extended Data Figure 5. Controls for optogenetic inhibition experiments.

a, AGRP neurons from *Agrp-ires-Cre; lsl-Halorhdopsin* (Halorhodopsin is expressed as a fusion protein with YFP) or *Agrp-ires-Cre; lsl-tdTomato* mice were dissociated and responses to light (LED-ON) were measured by whole-cell current clamp recordings. Representative examples (left) and the number of spikes measured (right) across animals before, during, and after photostimulation across mice, with normalization to the pre-illumination period, n=6 cells, mean ± s.e.m, lines: individual cells, **p<.01 by two-tailed Wilcoxon test (p pink PRE vs LIGHT: .03, p pink LIGHT vs POST: .03, p gray PRE vs

Author Manuscript Author Manuscript Author Manuscript Author Manuscript

LIGHT: .78, p gray LIGHT vs POST: .38). An additional statistical test involving one-way ANOVA with Tukey's multiple comparisons test revealed similar results (pink one-way ANOVA: p=.0003, with Tukey's multiple comparisons test: PRE vs LIGHT: p<.0001, LIGHT vs POST: p<.001, gray one-way ANOVA p=.53). **b**, Timeline and cartoon based on published brain section images[31] of optogenetic inhibition experiments in PVT. **c**, Investigation times in the two-choice behavioral assay during arcuate nucleus illumination in *Agrp-ires-Cre* (control) or *Agrp-ires-Cre; lsl-halorhodopsin* (ARC-OFF) mice, n=6 mice, mean ± s.e.m, lines with triangles: individual mice, *p<.05 by two-tailed Wilcoxon test (p control: .03; p ARC-OFF: .44). **d**, Food consumption after the two-choice odor test (FOOD 1 in timeline) in *Agrp-ires-Cre* (control) or *Agrp-ires-Cre; lsl-halorhodopsin* (ARC-OFF, PVT-OFF) mice during ARC (left) or PVT (right) illumination, n=6 mice, mean ± s.e.m, lines with triangles: individual mice, *p<.05 by two-tailed Mann–Whitney *U* test (p left: .015, p right: .57).

Author Manuscript
Author Manuscript
Author Manuscript
Author Manuscript

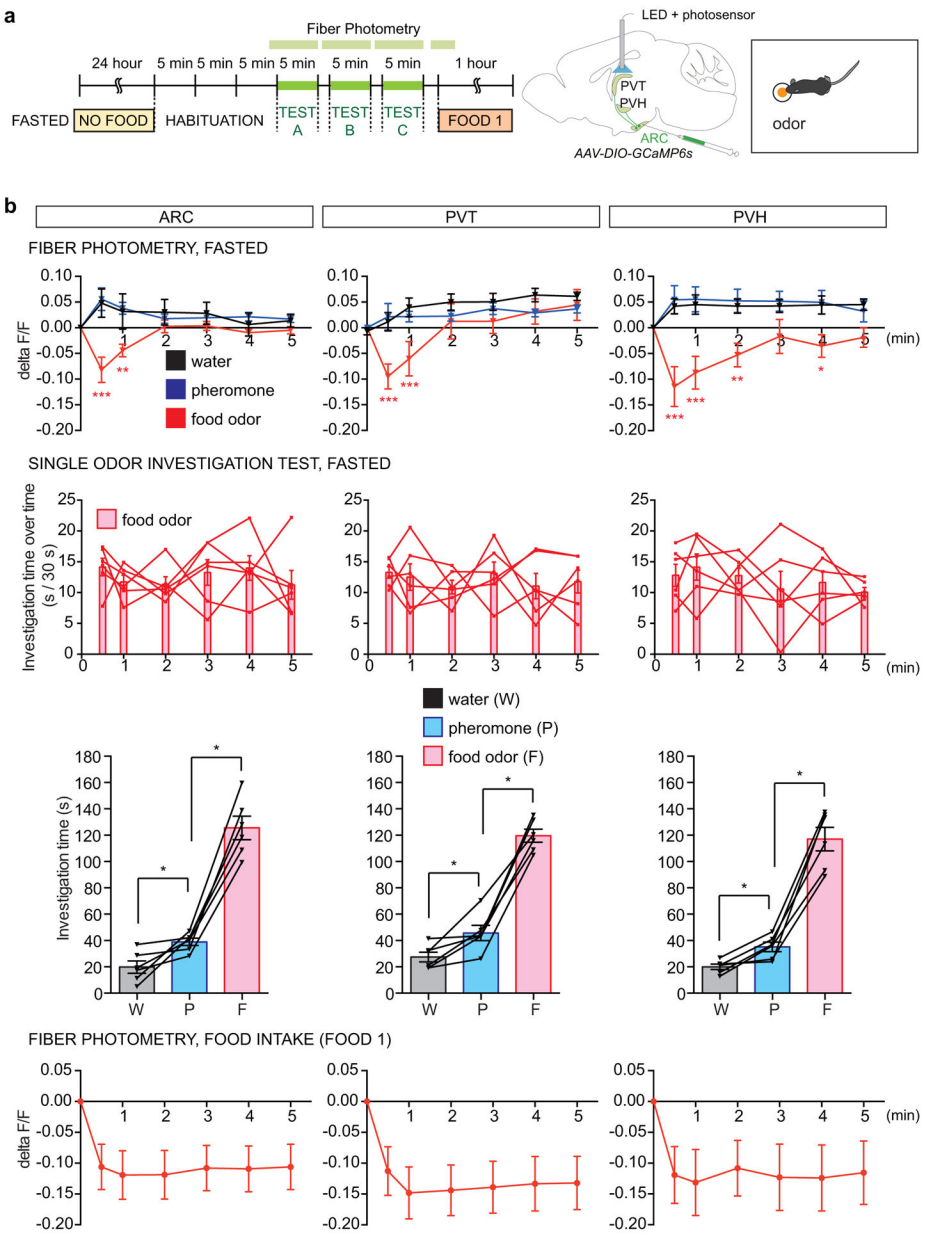

Extended Data Figure 6. Food odor investigation persists beyond transient AGRP neuron activity decreases measured by fiber photometry.

a, Timeline and depiction of fiber photometry experiments during single odor investigation, with cartoon based on published brain section images[31]. *Agrp-ires-Cre* mice were injected in the arcuate nucleus (ARC) with *AAV-DIO-GCaMP6s*, and fiber photometry was performed in the ARC, PVT or PVH during water investigation (TEST A), pheromone investigation (TEST B), food odor investigation (TEST C), and food consumption (FOOD 1). **b**, Changes in GCaMP6s fluorescence (delta F/F) were recorded by fiber photometry in brain regions indicated during single odor investigation (top row). Responses are depicted as the mean of measurements made in indicated time intervals (0–30 seconds, 30–60 seconds, or each subsequent minute), n=6 mice, mean ± s.e.m, *p<.05, **p<.01, ***p<.001, statistical comparisons between food odor and water responses by two-way ANOVA with Dunnett's

Author Manuscript Author Manuscript Author Manuscript Author Manuscript

multiple comparison. Food odor investigation time per 30 seconds (second row) during fiber photometry measurements above at time intervals (0–30 seconds, 30–60 seconds, or each subsequent minute), n=6 mice, mean ± s.e.m, lines: individual mice. Total investigation time for food odor, pheromones, and water during 5 minute fiber photometry test (third row), n=6 mice, mean ± s.e.m, lines with triangles: individual mice, *p<.05 by two-tailed Wilcoxon test (p water vs pheromone: .03; p pheromone vs food odor: .03 for ARC, PVT, PVH). Changes in GCaMP6s fluorescence (delta F/F) were recorded by fiber photometry during food consumption (FOOD 1 in timeline of **a**) after odor tests in the same mice (bottom row).

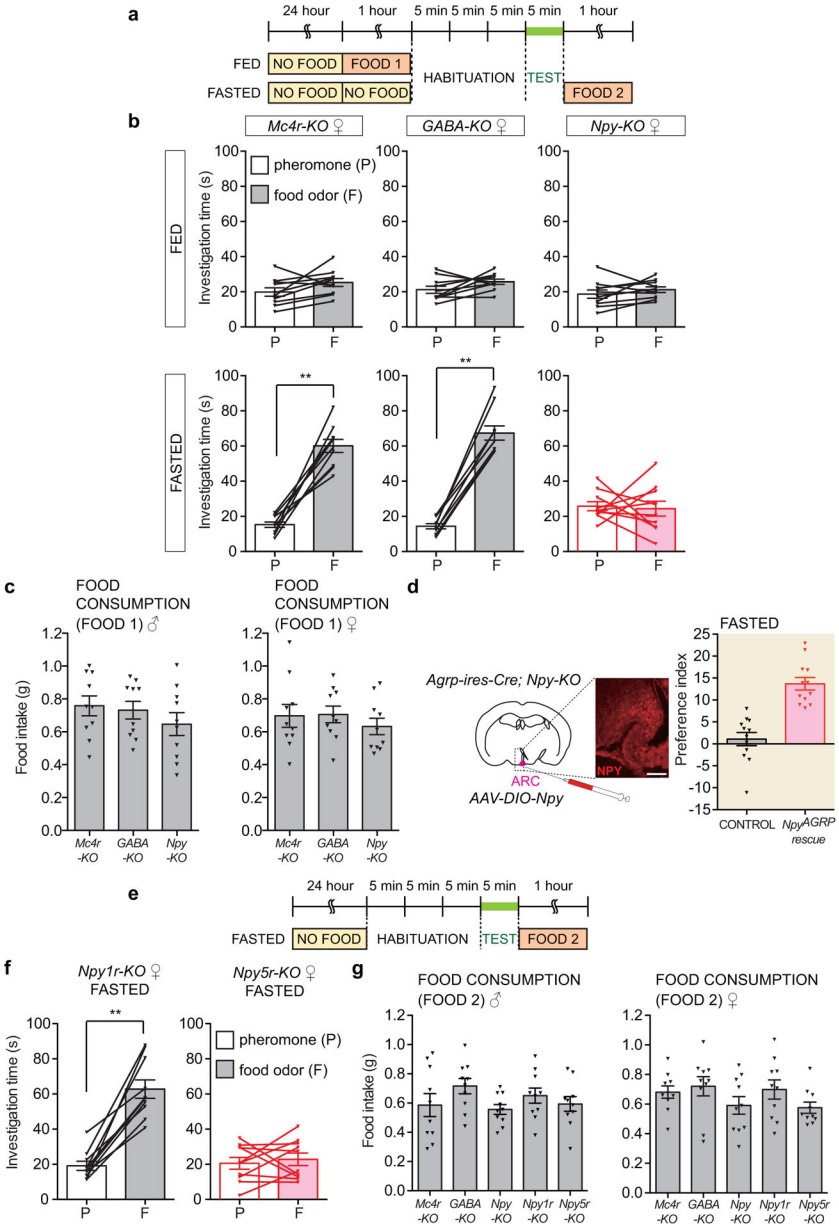

Extended Data Figure 7. Odor preferences and food consumption patterns in knockout and rescue mice.

Author Manuscript Author Manuscript Author Manuscript Author Manuscript

a, Timeline of two-choice behavioral assay. **b**, Investigation times for pheromones and food odors in fed (top) and fasted (bottom) knockout female mice indicated, n=10 mice, mean ± s.e.m, lines with triangles: individual mice, **p<.01 by two-tailed Wilcoxon test (from left to right, p fed: .08, .16, .24; p fasted: .002, .002, .85). **c**, Food intake prior to two-choice assay (FOOD 1 in timeline) of various knockout male (left) and female (right) mice (n=10 mice, mean ± s.e.m, triangles: individual mice). **d**, Cartoon (left) and preference indices (right) of NPY rescue experiments involving *Npy-KO* (control) and *Agrp-ires-Cre; Npy-KO* (Npy^{AGRP} rescue) mice three weeks after *AAV-lsl-Npy* injection in the arcuate nucleus. Brain cartoon is based on published brain section images[31] NPY immunohistochemistry is depicted in the figure inset. Preference indices are derived from data in Fig. 3d (n=12 mice, males and females, mean ± s.e.m, scale bar: 100 μm). **e**, Timeline of two-choice behavioral assay for receptor knockouts. **f**, Investigation times for pheromones and food odors in fasted knockout female mice indicated, n=10 mice, mean ± s.e.m, lines with triangles: individual mice, **p<.01 by two-tailed Wilcoxon test (p *Npy1r-KO*: .02; p *Npy5r-KO*: .77). **g**, Food intake after two-choice assay (FOOD 2 in timeline) of indicated knockout male and female mice (n=10 mice, mean ± s.e.m, triangles: individual mice).

Author Manuscript Author Manuscript Author Manuscript Author Manuscript

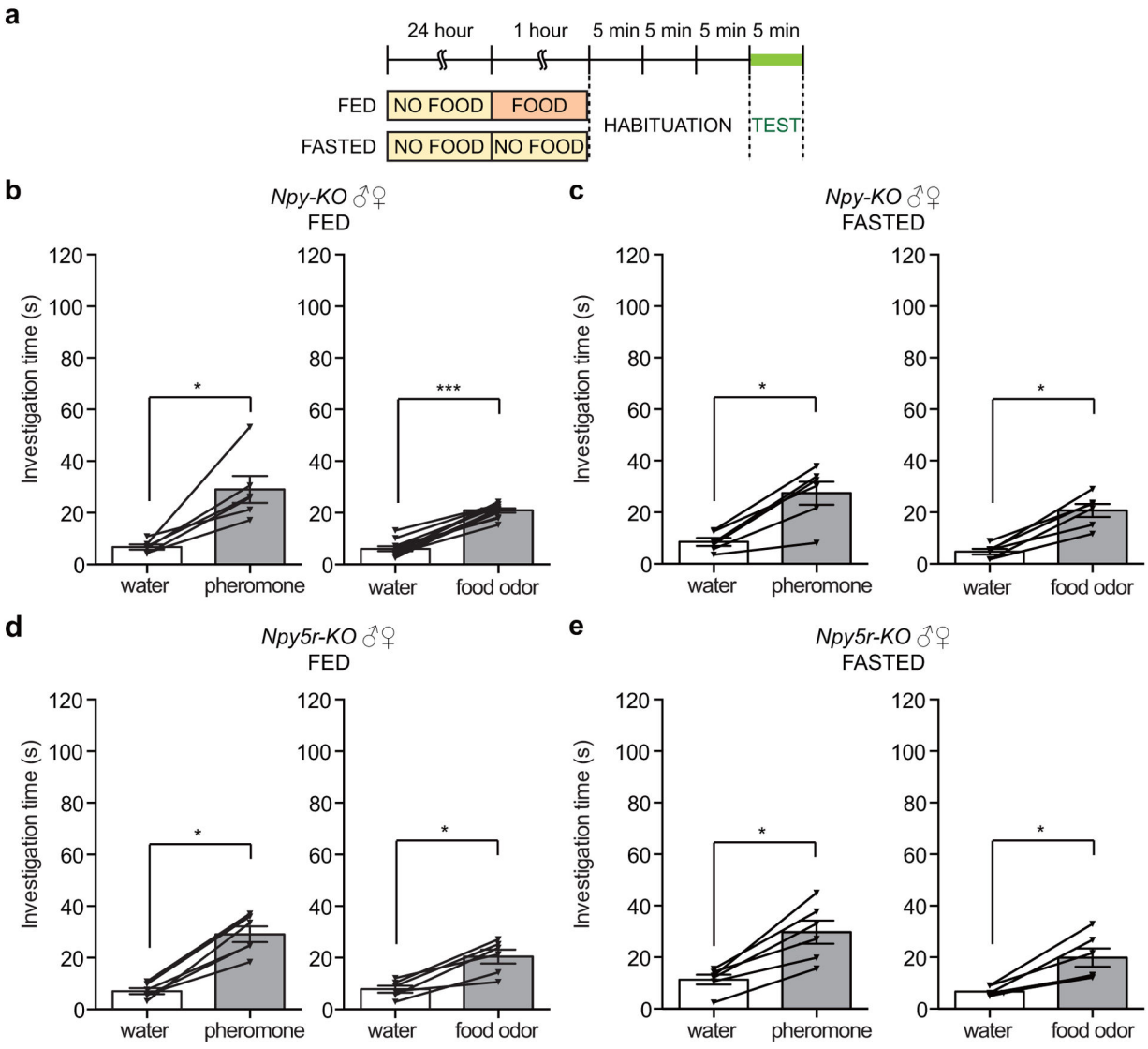

Extended Data Figure 8. Single odor preference assays in knockout mice.

a, Timeline of behavioral assay. **b-e**, Odor investigation times of fed *Npy-KO* (**b**), fasted *Npy-KO* (**c**), fed *Npy5r-KO* (**d**) and fasted *Npy5r-KO* (**e**) mice in single odor pairings with water, n=3 males and 3 females, mean ± s.e.m, lines with triangles: individual mice, *p<.05, **p<.01 by two-tailed Wilcoxon test (p values for **b**: .03, .001, **c**: .03, .03, **d**: .03, .03, **e**: .03, .03.

Author Manuscript Author Manuscript Author Manuscript Author Manuscript

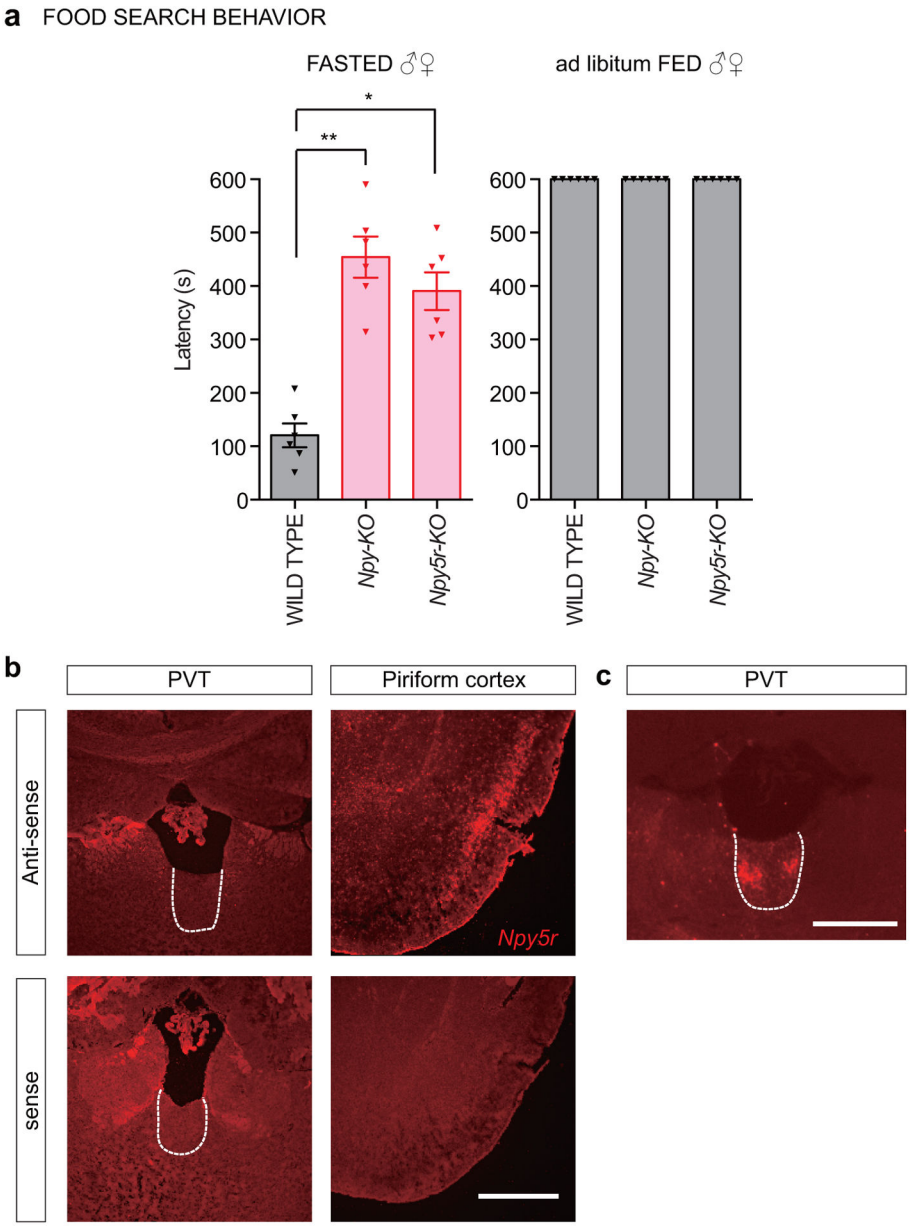

Extended Data Figure 9. Food search behavior in knockout mice and analysis of *Npy5r* expression.

a, Latency to discover a food pellet buried in bedding was timed in fasted (left) and fed (right) mice indicated (n=3 males and 3 females, mean ± s.e.m, **p<.01, *p<.05 by Kruskal–Wallis test with Dunn's multiple comparison). **b**, RNA *in situ* hybridization using *Npy5r* anti-sense and sense probes in coronal brain cryosections with PVT (left, dashed lines) and piriform cortex, scale bar: 500 μm. **c**, AGRP neuron projections to the PVT were visualized by immunohistochemistry for tdTomato in *Agrp-ires-Cre* mice injected in the arcuate nucleus with *AAV-DIO-tdTomato*, scale bar: 500 μm. Images in **b** and **c** are representative of three independent experiments involving different mice.

Author Manuscript Author Manuscript Author Manuscript Author Manuscript

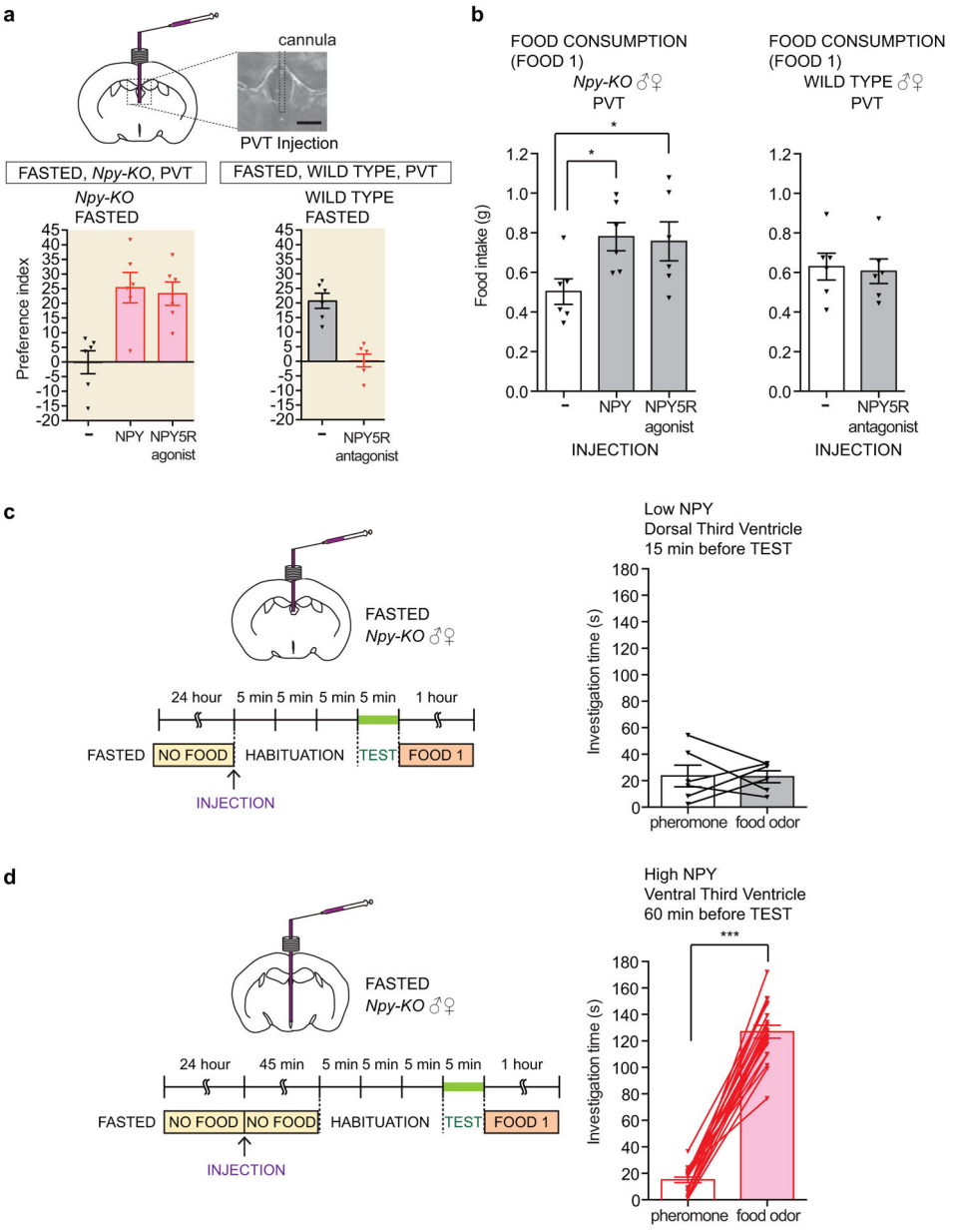

Extended Data Figure 10. Controls for NPY injection into PVT.

a, Cartoon depicting injection site (top) and preference indices for experiments in Fig 3h and 3i (n=10 males and 10 females, mean + s.e.m.). **b**, Post-test food consumption (FOOD 1) for mice in Fig 3h and 3i, n=6 (3 males, 3 females), mean ± s.e.m, triangles: individual mice, *p<.05 by two-tailed Mann–Whitney *U* test (p NPY vs control: .015, p NPY5R agonist vs control: .04). **c**, Fasted *Npy-KO* mice were injected with low NPY levels (0.02 mg/kg) in the dorsal third ventricle, and after 15 minutes behavior was analyzed in the two-choice odor preference assay, n=6 (3 males, 3 females), mean ± s.e.m, lines with triangles: individual mice, p>.99 by two-tailed Wilcoxon test. **d**, Fasted *Npy-KO* mice were injected with high NPY levels (0.2 mg/kg) in the ventral third ventricle, and after 60 minutes behavior was analyzed in the two-choice odor preference assay, n=20 (10 males, 10 females), mean ±

Author Manuscript Author Manuscript Author Manuscript Author Manuscript

s.e.m, lines with triangles: individual mice, ***p<.001 by two-tailed Wilcoxon test. Brain cartoons are based on published brain section images[31].

Supplementary Material

Refer to Web version on PubMed Central for supplementary material.

Acknowledgments

We thank Brad Lowell, Mark Andermann, Sandeep Datta, Mark Albers, John Flanagan, Chen Ran, and Ken Tao for manuscript comments, Qian Li and Ken Tao for experimental assistance, and the Nikon Imaging Center at Harvard Medical School for microscopy assistance. The work was supported by an NIH grant to SDL (R01 DC013289) and a Uehara Memorial Foundation postdoctoral fellowship and Mishima Kaiun Memorial Foundation funding to NH. SDL is an investigator of the Howard Hughes Medical Institute.

References

1. Li Q & Liberles SD Aversion and Attraction through Olfaction. Curr Biol 25, R120–R129, doi:10.1016/j.cub.2014.11.044 (2015). [PubMed: 25649823]
2. Andermann ML & Lowell BB Toward a Wiring Diagram Understanding of Appetite Control. Neuron 95, 757–778, doi:10.1016/j.neuron.2017.06.014 (2017). [PubMed: 28817798]
3. Sternson SM Hypothalamic survival circuits: blueprints for purposive behaviors. Neuron 77, 810–824, doi:S0896–6273(13)00176–1 [pii] 10.1016/j.neuron.2013.02.018 (2013). [PubMed: 23473313]
4. Rolls ET Taste, olfactory, and food reward value processing in the brain. Progress in neurobiology 127–128, 64–90, doi:10.1016/j.pneurobio.2015.03.002 (2015).
5. Tong J et al. Ghrelin enhances olfactory sensitivity and exploratory sniffing in rodents and humans. J Neurosci 31, 5841–5846, doi:10.1523/JNEUROSCI.5680-10.2011 (2011). [PubMed: 21490225]
6. Negroni J et al. Neuropeptide Y enhances olfactory mucosa responses to odorant in hungry rats. PLoS One 7, e45266, doi:10.1371/journal.pone.0045266 (2012). [PubMed: 23024812]
7. Soria-Gomez E et al. The endocannabinoid system controls food intake via olfactory processes. Nature neuroscience 17, 407–415, doi:10.1038/nn.3647 (2014). [PubMed: 24509429]
8. Root CM, Ko KI, Jafari A & Wang JW Presynaptic facilitation by neuropeptide signaling mediates odor-driven food search. Cell 145, 133–144, doi:S0092–8674(11)00122-X [pii] 10.1016/j.cell.2011.02.008 (2011). [PubMed: 21458672]
9. Li Q et al. Synchronous evolution of an odor biosynthesis pathway and behavioral response. Curr Biol 23, 11–20, doi:S0960–9822(12)01268–7 [pii] 10.1016/j.cub.2012.10.047 (2013). [PubMed: 23177478]
10. Burnett CJ et al. Need-based prioritization of behavior. Elife 8, doi:10.7554/eLife.44527 (2019).
11. Aponte Y, Atasoy D & Sternson SM AGRP neurons are sufficient to orchestrate feeding behavior rapidly and without training. Nature neuroscience 14, 351–355, doi:nn.2739 [pii] 10.1038/nn.2739 (2011). [PubMed: 21209617]
12. Krashes MJ et al. Rapid, reversible activation of AgRP neurons drives feeding behavior in mice. J Clin Invest 121, 1424–1428, doi:46229 [pii] 10.1172/JCI46229 (2011). [PubMed: 21364278]
13. Luquet S, Perez FA, Hnasko TS & Palmiter RD NPY/AgRP neurons are essential for feeding in adult mice but can be ablated in neonates. Science (New York, N.Y 310, 683–685 (2005).
14. Alhadeff AL et al. A Neural Circuit for the Suppression of Pain by a Competing Need State. Cell 173, 140–152 e115, doi:10.1016/j.cell.2018.02.057 (2018). [PubMed: 29570993]
15. Betley JN, Cao ZF, Ritola KD & Sternson SM Parallel, redundant circuit organization for homeostatic control of feeding behavior. Cell 155, 1337–1350, doi:10.1016/j.cell.2013.11.002 (2013). [PubMed: 24315102]
16. Essner RA et al. AgRP Neurons Can Increase Food Intake during Conditions of Appetite Suppression and Inhibit Anorexigenic Parabrachial Neurons. J Neurosci 37, 8678–8687, doi:10.1523/JNEUROSCI.0798-17.2017 (2017). [PubMed: 28821663]

Author Manuscript Author Manuscript Author Manuscript Author Manuscript

17. Padilla SL et al. Agouti-related peptide neural circuits mediate adaptive behaviors in the starved state. Nature neuroscience 19, 734–741, doi:10.1038/nn.4274 (2016). [PubMed: 27019015]
18. Small DM, Veldhuizen MG, Felsted J, Mak YE & McGlone F Separable substrates for anticipatory and consummatory food chemosensation. Neuron 57, 786–797, doi:10.1016/j.neuron.2008.01.021 (2008). [PubMed: 18341997]
19. Rousseaux M, Muller P, Gahide I, Mottin Y & Romon M Disorders of smell, taste, and food intake in a patient with a dorsomedial thalamic infarct. Stroke 27, 2328–2330 (1996). [PubMed: 8969802]
20. Betley JN et al. Neurons for hunger and thirst transmit a negative-valence teaching signal. Nature 521, 180–185, doi:10.1038/nature14416 (2015). [PubMed: 25915020]
21. Chen Y, Lin YC, Kuo TW & Knight ZA Sensory detection of food rapidly modulates arcuate feeding circuits. Cell 160, 829–841, doi:10.1016/j.cell.2015.01.033 (2015). [PubMed: 25703096]
22. Krashes MJ, Shah BP, Koda S & Lowell BB Rapid versus delayed stimulation of feeding by the endogenously released AgRP neuron mediators GABA, NPY, and AgRP. Cell Metab 18, 588–595, doi:10.1016/j.cmet.2013.09.009 (2013). [PubMed: 24093681]
23. Chen Y et al. Sustained NPY signaling enables AgRP neurons to drive feeding. Elife 8, doi:10.7554/eLife.46348 (2019).
24. Krashes MJ et al. A neural circuit mechanism integrating motivational state with memory expression in Drosophila. Cell 139, 416–427, doi:S0092–8674(09)01105–2 [pii] 10.1016/j.cell.2009.08.035 (2009). [PubMed: 19837040]
25. Kay LM & Sherman SM An argument for an olfactory thalamus. Trends in neurosciences 30, 47–53, doi:10.1016/j.tins.2006.11.007 (2007). [PubMed: 17161473]
26. Tham WW, Stevenson RJ & Miller LA The functional role of the medio dorsal thalamic nucleus in olfaction. Brain research reviews 62, 109–126, doi:10.1016/j.brainresrev.2009.09.007 (2009). [PubMed: 19800366]
27. Otis JM et al. Paraventricular Thalamus Projection Neurons Integrate Cortical and Hypothalamic Signals for Cue-Reward Processing. Neuron, doi:10.1016/j.neuron.2019.05.018 (2019).
28. Zhu Y et al. Dynamic salience processing in paraventricular thalamus gates associative learning. Science (New York, N.Y 362, 423–429, doi:10.1126/science.aat0481 (2018).
29. Livneh Y et al. Homeostatic circuits selectively gate food cue responses in insular cortex. Nature 546, 611–616, doi:10.1038/nature22375 (2017). [PubMed: 28614299]
30. Kirouac GJ Placing the paraventricular nucleus of the thalamus within the brain circuits that control behavior. Neuroscience and biobehavioral reviews 56, 315–329, doi:10.1016/j.neubiorev.2015.08.005 (2015). [PubMed: 26255593]
31. Franklin K & Paxinos G The mouse brain in stereotaxic coordinates. (Academic Pres, 2008).
32. Ben-Shaul Y OptiMouse: a comprehensive open source program for reliable detection and analysis of mouse body and nose positions. BMC Biol 15, 41, doi:10.1186/s12915-017-0377-3 (2017). [PubMed: 28506280]

Author Manuscript Author Manuscript Author Manuscript Author Manuscript

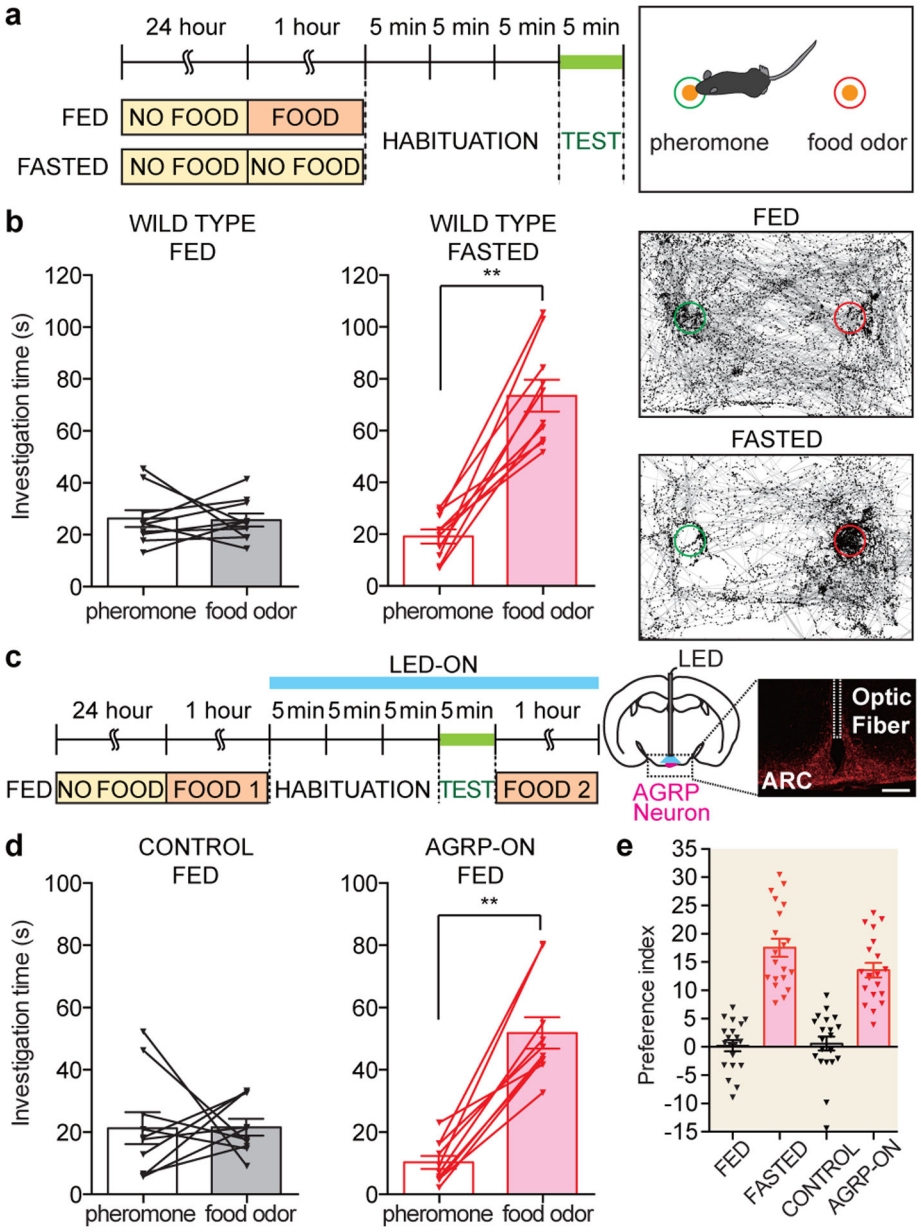

Figure 1. Hunger and AGRP neuron activation promote attraction to food odors over pheromones.

a, Timeline and cartoon of two-choice behavioral assay. **b**, Investigation time (left) of fed and fasted male wild type mice to pheromones and food odors. Behavior of representative mice (right) where nose position is traced (black) over the 5 minute trial. **c**, Timeline (left) of two-choice assay involving AGRP neuron optogenetics, with location of optic fiber depicted in a cartoon (right) drawn based on published brain section images[31], scale bar: 200 μm. **d**, Investigation time of fed control and fed AGRP-ON male mice to pheromones and food odors. **e**, Preference indices for food odors over pheromones in animals indicated. (n=10 mice except **e**: n= 10 males and 10 females, mean ± s.e.m, lines with triangles: individual mice, **p<.01 by two-tailed Wilcoxon test).

Author Manuscript Author Manuscript Author Manuscript Author Manuscript

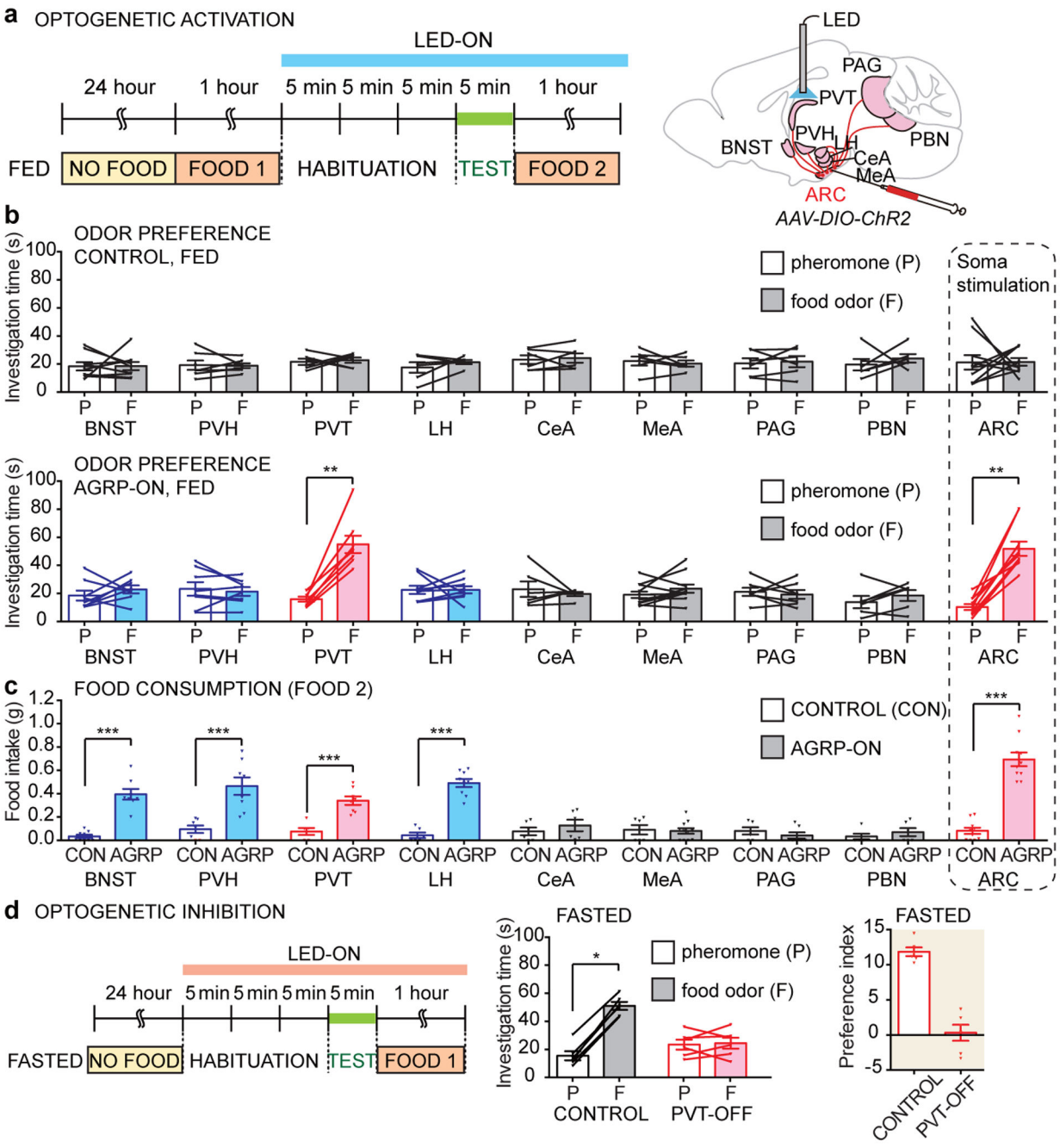

Figure 2. Thalamic AGRP neuron projections promote food odor attraction.

a, Timeline of two-choice assay involving AGRP neuron optogenetic stimulation (blue bar), with optic fiber location depicted in a cartoon based on published brain section images[31]. **b**, Investigation time of fed control (top) and fed AGRP-ON (bottom) mice to pheromones (P) and food odors (F) following optogenetic stimulation of AGRP axon terminals in brain regions indicated. **c**, Food consumption after the two-choice odor test (FOOD 2 in timeline) in fed control and fed AGRP-ON mice following illumination of brain regions indicated. **d**, Timeline (left), investigation times (middle) and preference index (right) for optogenetic inhibition experiments involving PVT illumination. (n: mice used for control, AGRP-ON in

Author Manuscript Author Manuscript Author Manuscript Author Manuscript

b-c: BNST: 9, 8; PVH: 7, 8; PVT: 6, 8; LH: 6, 9; CeA: 6, 6; MeA: 6, 11; PAG: 6, 7; PBN: 6, 6; ARC: 10,10, n in **d**: 6 mice, males and females, mean ± s.e.m, lines: individual mice, *p<.05, **p<.01, ***p<.001 by two-tailed Wilcoxon test except for **c** by two-tailed Mann–Whitney *U* test).

Author Manuscript Author Manuscript Author Manuscript Author Manuscript

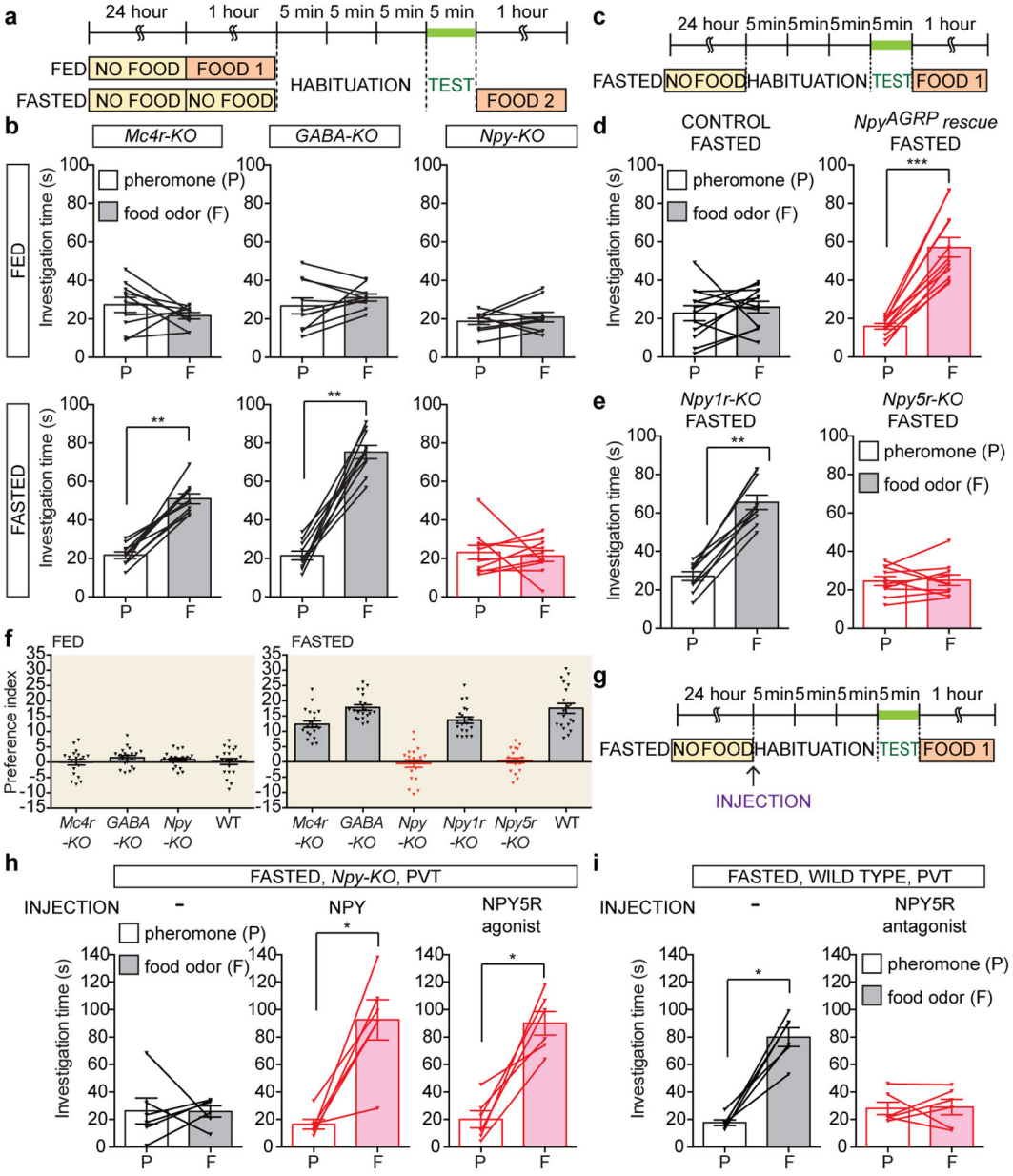

Figure 3. NPY and NPY5R are required for hunger-dependent food odor attraction.

a-b, Timeline (**a**) and odor investigation times (**b**) in fed and fasted knockout male mice indicated, n=10 mice, males and females, mean ± s.e.m, lines with triangles: individual mice. **c-d**, Timeline (**c**) and odor investigation times (**d**) in *Npy-KO* (control) and *Agrp-ires-Cre; Npy-KO* (*Npy*^{AGRP} rescue) mice three weeks after *AAV-DIO-Npy* injection in the arcuate nucleus, n=12 mice, males and females, mean ± s.e.m, lines with triangles: individual mice. **e-f**, Investigation times (**e**) and odor preference indices (**f**) for fed and fasted knockout mice indicated, n=10 mice except preference index: n=10 males and 10 females, mean ± s.e.m, lines with triangles: individual mice). **g-h**, Timeline (**g**) and odor investigation times (**h**) for fasted *Npy-KO* mice injected in the PVT with artificial cerebrospinal fluid (aCSF) alone (−), NPY (0.02 mg/kg in aCSF) or NPY5R agonist ([CPP$^{1–7}$, NPY$^{19–23}$,

Author Manuscript Author Manuscript Author Manuscript Author Manuscript

Ala[31], Aib[32], Gln[34]-hPancreatic Polypeptide, 0.002 mg/kg in aCSF), n=3 males and 3 females, mean ± s.e.m, lines with triangles: individual mice. **i**, Investigation times for fasted wild-type mice injected in the PVT with aCSF alone (−) or NPY5R antagonist (CGP71683, 0.2 mg/kg in aCSF), n=3 males and 3 females, mean ± s.e.m, lines with triangles: individual mice. *p<.05, **p<.01, ***p<.001 by two-tailed Wilcoxon test.